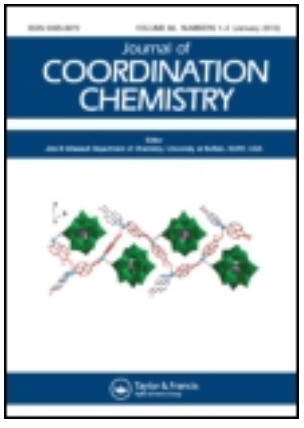

Journal of Coordination Chemistry
Publication details, including instructions for authors and subscription information:
http://www.tandfonline.com/loi/gcoo20

Liquid-crystalline oxovanadium(IV) complexes accessed from bidentate [N, O] donor salicylaldimine Schiff-base ligands

Chira R. Bhattacharjee [a], Gobinda Das [a] & Paritosh Mondal [a]
[a] Department of Chemistry, Assam University, Silchar 788011, Assam, India
Published online: 27 Sep 2011.

To cite this article: Chira R. Bhattacharjee, Gobinda Das & Paritosh Mondal (2011) Liquid-crystalline oxovanadium(IV) complexes accessed from bidentate [N, O] donor salicylaldimine Schiff-base ligands, Journal of Coordination Chemistry, 64:18, 3273-3289, DOI: 10.1080/00958972.2011.619262

To link to this article: http://dx.doi.org/10.1080/00958972.2011.619262

Journal of Coordination Chemistry
Vol. 64, No. 18, 20 September 2011, 3273–3289

Liquid-crystalline oxovanadium(IV) complexes accessed from bidentate [N, O] donor salicylaldimine Schiff-base ligands

CHIRA R. BHATTACHARJEE*, GOBINDA DAS and PARITOSH MONDAL

Department of Chemistry, Assam University, Silchar 788011, Assam, India

(*Received 11 July 2011; in final form 22 August 2011*)

A series of bis[4-(*n*-alkoxy)-N-(4′-R-phenyl)salicylideneiminato]oxovanadium(IV) complexes ($n = 6, 10, 14, 16, 18$ and $R = C_3H_7$) were prepared and their mesogenic properties were investigated. The mesomorphic behaviors of the compounds were studied by polarized optical microscopy and differential scanning calorimetry. Ligands display SmA/SmC and unexpected nematic mesophases. The complexes bearing longer alkoxy carbon chain ($n = 10, 14, 16$, and 18) showed both monotropic or enantiotropic transitions with smectic A and high ordered smectic E phases. However, the complex with shorter carbon chain length ($n = 6$) showed monotropic transition with an unprecedented nematic (N) phase. A density functional theory study was carried out using DMol3 at BLYP/DNP level to obtain a stable optimized structure. A square-pyramidal geometry for the vanadyl complexes has been suggested. A $\nu_{V=O}$ stretching value of $\sim 970\,cm^{-1}$ corroborated absence of any $V=O\cdots V=O$ interactions. Cyclic voltammetry revealed a quasireversible one-electron response at 0.61 V for the VO(IV)–VO(V) redox couple. Variable temperature magnetic susceptibility measurements of the vanadyl complexes suggested absence of any exchange interactions among the vanadyl spin centers.

Keywords: Vanadium; Metallomesogen; Schiff bases; DFT

1. Introduction

Metal containing liquid crystals are a promising area of current research owing to the possibility of combining the optical, electronic, and magnetic properties of transition metal complexes with properties of anisotropic fluids [1–3]. The presence of the metal ion can produce different assembly structures, leading to interesting liquid-crystalline properties [1–15]. Coordination compounds of redox active metals that exhibit paramagnetism can produce novel conductors, magneto-optic data storage, and display devices [16]. Oxovanadium(IV) complexes of Schiff-base ligands received significant attention in the context of antimicrobial [17–19], antitumor [20], antileukemia [21], spermicidal [22], and insulin mimetic activities [23–25]. Unlike other transition metals, the presence of dative bonding between oxovanadium(IV) cores often lead to polymeric $V=O\cdots V=O\cdots$ chain formation. Due to such properties, oxovanadium complexes are quite significant as novel ferroelectric/piezoelectric and NLO materials [26]. In addition, selective epoxidation of olefins catalyzed by vanadium Schiff-base complexes

*Corresponding author. Email: crbhattacharjee@rediffmail.com

ISSN 0095-8972 print/ISSN 1029-0389 online
DOI: 10.1080/00958972.2011.619262

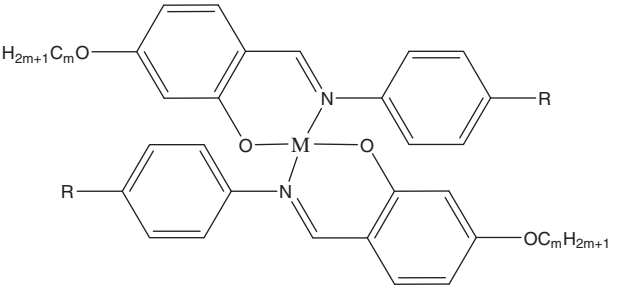

Figure 1. Structure of N-(4-alkoxysalicylidene)-4′-alkylaniline complex.

are one of the most important industrial processes [20–22]. More recently vanadium coordination compounds were shown to catalyze the selective oxidation of alkenes by molecular oxygen [27]. Schiff-base vanadium complexes also serve as very interesting model compounds for several biochemical processes [28–30]. Metal complexes derived from the salicylaldimines feature among the earliest and most widely studied class of metallomesogens [1–15]. The advantages of incorporating an imine functionality lie in the versatility, structural variety, ease of preparation, and derivatization of such groups. In the past few years, a wide variety of metallomesogens has been synthesized based on salicylaldimine ligands [31–41]. First reports on mesogenic vanadyl complexes with salicylaldimine ligands were made by Galyametdinov *et al*. [42]. Later Ghedini and co-workers [43–47] investigated a series of N-(4-alkoxysalicylidene)-4′-alkylaniline copper and vanadium complexes (figure 1). The ligands showed SmC/SmA/N phases, however, all complexes showed the SmA mesophase. Very recently we reported a series of analogous oxovanadium(IV) complexes that showed smectic mesomorphism [48, 49]. As for the vanadyl complexes, the mesophase became destabilized with respect to that of the copper complexes, probably due to the distorted square-pyramidal geometry around the metal center [43–49]. In our earlier observation, we noticed that complexes bearing alkoxy and polar substituents on aniline opposite to the imine linkage exhibited a smectic mesomorphism [47–49]. The formation of smectic phases (SmA and SmC) was favored in this type of complex. Bis[4-(n-alkoxy)-N-(4′-R-phenyl)salicylideneiminato] oxovanadium(IV) complexes (R = alkyl or polar group and alkoxy) reported earlier showed only smectic mesomorphism [47–49].

Our goal in this study is to devise a newer series of oxovanadium(IV) Schiff-base complexes containing both shorter and longer alkoxy substituents on one side of the ligand with the other side bearing a fixed alkyl group (figure 1). All the complexes with carbon length ($n = 10, 14, 16, 18$) revealed SmA and SmE mesophases while the complex with $n = 6$ exhibited a nematic (N) phase.

2. Experimental

2.1. *Materials*

All solvents were purified and dried using standard procedures. The materials were procured from Tokyo Kasei, Japan and Lancaster Chemicals, USA.

Silica (60–120 mesh) from Spectrochem was used for chromatographic separation. Silica gel G (E-merck, India) was used for TLC.

2.2. *Techniques*

C, H, and N analyses were carried out using a PE2400 elemental analyzer. Molar conductances of the compounds were determined in CH_2Cl_2 (*ca* 10^{-3} mol L^{-1}) at room temperature using a MAC-554 conductometer. ^1H NMR spectra were recorded on a Bruker DPX-300 spectrometer in $CDCl_3$ with TMS as internal standard. UV-Vis absorption spectra of the compounds in CH_2Cl_2 were recorded on a Shimadzu UV-160PC spectrophotometer. Infrared spectra were recorded on a Perkin-Elmer L 120-000 A spectrometer as KBr discs. The mesomorphic textures of the compounds were studied using a polarizing microscope (Nikon optiphot-2-pol) attached with Instec hot and cold stage HCS302, STC200 temperature controller configured for HCS302. The accuracies in temperatures are 0.1°C. The thermal behaviors of the compounds were studied using a Perkin-Elmer differential scanning calorimeter (DSC) Pyris-1 spectrometer with a heating or cooling rate of 5°C min^{-1}. DC magnetic susceptibility data were collected on a Vibrating Sample Magnetometer, Physical Property Measurement System (PPMS Quantum Design, USA) in the temperature range 2.5–300 K with applied field of 100 Oe. Electrochemical measurements were performed using computer-controlled CHI 660 C electrochemical workstation with Pt-disc electrodes. All measurements were carried out under nitrogen at 298 K with reference to SCE in acetonitrile using $[n\mathrm{Bu_4N}][\mathrm{ClO_4}]$ as supporting electrolyte.

2.3. *Synthesis and analyses*

2.3.1. Synthesis of *n*-alkoxysalicylaldehyde ($n = 6, 10, 14, 16, 18$). Alkoxysalicylaldehyde derivatives were prepared following the general method described, scheme 1 [48, 49]. 2,4-Dihydroxybenzaldehyde (10 mmol, 1.38 g), $KHCO_3$ (10 mmol, 1 g), KI (catalytic amount), and 1-bromohexane (10 mmol, 1.6 g), 1-bromodecane (10 mmol, 2.2 g), 1-bromotetradecane (10 mmol, 2.7 g), 1-bromohexadecane (10 mmol, 3.0 g), or 1-bromooctaadecane (10 mmol, 3.3 g) were mixed in 250 mL of dry acetone. The mixture was heated under reflux for 24 h, and then filtered, while hot, to remove any insoluble solids. Dilute HCl was added to neutralize the warm solution, which was then extracted with chloroform (100 mL). The combined chloroform extract was concentrated to give a purple solid. The solid was purified by column chromatography using a mixture of chloroform and hexane (v/v, 1/1) as eluent. Evaporation of the solvents afforded a white solid product.

2.3.2. 4-*n*-hexyloxysalicylaldehyde. Yield: 5 g, 86%. Anal. for $C_{13}H_{18}O_3$: FAB mass (*m*/*e*, fragment): *m*/*z*: calcd 222.1; found: 223 $[M + H^+]$. ^1H NMR (400 MHz, $CDCl_3$): 0.94 (t, $J = 5.6$, 3H, CH_3), 1.23–1.73 (m, 8H, $(CH_2)_4$), 3.97 (t, $J = 5.9$, 2H, OCH_2), 7.5 (d, $J = 7.2$, 1H, H-aryl), 5.9 (s, 1H, OH), 10.6 (s, 1H, −CHO); ^{13}C NMR (75.45 MHz; $CDCl_3$; Me_4Si at 25°C, ppm) $\delta = 107.3$ (−C1), 131.3 (−C2), 103.7 (−C3), 165.5 (−C4), 188.7 (−C10). IR (ν_{max}, cm^{-1}, KBr): 3425(νOH), 2915 ($\nu as_{(C-H)}$, CH_2), 2860 ($\nu s_{(C-H)}$, CH_2), 1625 ($\nu_{CH=0}$), 1275 (ν_{C-O}).

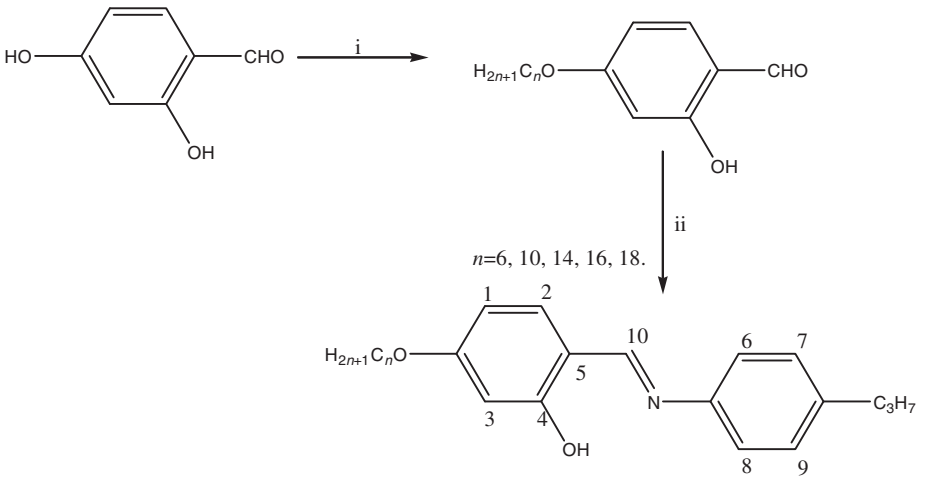

$n = 6$, 4-6-3; $n = 10$, 4-10-3; $n = 14$, 4-14-3; $n = 16$, 4-16-3; $n = 18$, 4-18-3.

Scheme 1. i: $C_nH_{2n+1}Br$, $KHCO_3$, KI, dry acetone, Δ, 40 h; ii: glacial AcOH, absolute EtOH Δ, 4 h.

2.3.3. 4-*n*-decyloxysalicylaldehyde. Yield: 5 g, 80%. Anal. for $C_{17}H_{26}O_3$: FAB mass (*m*/*e*, fragment): *m*/*z*: calcd 278.1; found: 279 $[M + H^+]$. ^1H NMR (400 MHz, $CDCl_3$): 0.96 (t, $J = 5.7$, 3H, CH_3), 1.21–1.74 (m, 16H, $(CH_2)_8$), 3.97 (t, $J = 5.9$, 2H, OCH_2), 7.5 (d, $J = 7.2$, 1H, H-aryl), 5.9 (s, 1H, OH), 10.6 (s, 1H, -CHO); ^{13}C NMR (75.45 MHz; $CDCl_3$; Me_4Si at 25°C, ppm) $\delta = 107.3$ (−C1), 131.1 (−C2), 103.9 (−C3), 165.6 (−C4), 188.8 (−C10). IR (ν_{max}, cm^{-1}, KBr): 3425 (νOH), 2915 ($\nu as_{(C-H)}$, CH_2), 2860 ($\nu s_{(C-H)}$, CH_2), 1625 ($\nu_{CH=0}$), 1275 (ν_{C-O}).

2.3.4. 4-*n*-tetradecyloxysalicylaldehyde. Yield: 3.5 g, 88%. Anal. for $C_{21}H_{34}O_3$: FAB mass (*m*/*e*, fragment): *m*/*z*: calcd 334.2; found: 335 $[M + H^+]$. ^1H NMR (400 MHz, $CDCl_3$): 0.98 (t, $J = 5.7$, 3H, CH_3), 1.22–1.75 (m, 22H, $(CH_2)_{11}$), 3.95 (t, $J = 5.9$, 2H, OCH_2), 7.41 (d, $J = 7.2$, 1H, H-aryl), 5.81 (s, 1H, OH), 11.1 (s, 1H, −CHO); ^{13}C NMR (75.45 MHz; $CDCl_3$; Me_4Si at 25°C, ppm) $\delta = 107.3$ (−C1), 131.1 (−C2), 103.9 (−C3), 165.6 (−C4), 188.8 (−C10). IR (ν_{max}, cm^{-1}, KBr): 3425 (νOH), 2915 ($\nu as_{(C-H)}$, CH_2), 2865 ($\nu s_{(C-H)}$, CH_2), 1620 ($\nu_{CH=0}$), 1275 (ν_{C-O}).

2.3.5. 4-*n*-hexaadecyloxysalicylaldehyde. Yield: 5 g, 88%. Anal. for $C_{23}H_{38}O_3$: FAB mass (*m*/*e*, fragment): *m*/*z*: calcd 362.5; found: 363 $[M + H^+]$. ^1H NMR (400 MHz, $CDCl_3$): 0.97 (t, $J = 5.7$, 3H, CH_3), 1.23–1.71 (m, 28H, $(CH_2)_{14}$), 3.94 (t, $J = 5.9$, 2H, OCH_2), 7.42 (d, $J = 7.1$, 1H, H-aryl), 5.82 (s, 1H, OH), 11.4 (s, 1H, −CHO); ^{13}C NMR (75.45 MHz; $CDCl_3$; Me_4Si at 25°C, ppm) $\delta = 106.3$ (−C1), 131.1 (−C2), 102.9 (−C3), 165.6 (−C4), 187.8 (−C10). IR (ν_{max}, cm^{-1}, KBr): 3425 (νOH), 2915 ($\nu as_{(C-H)}$, CH_2), 2860 ($\nu s_{(C-H)}$, CH_2), 1620 ($\nu_{CH=0}$), 1275 (ν_{C-O}).

2.3.6. 4-*n*-octaadecyloxysalicylaldehyde. Yield: 5 g, 88%. Anal. for $C_{25}H_{42}O_3$: FAB mass (*m*/*e*, fragment): *m*/*z*: calcd 390.3; found: 391 $[M + H^+]$. ^1H NMR (400 MHz,

$CDCl_3$): 0.99 (t, $J = 5.7$, 3H, CH_3), 1.22–1.71 (m, 32H, $(CH_2)_{16}$), 3.95 (t, $J = 5.9$, 2H, OCH_2), 7.41 (d, $J = 7.1$, 1H, H-aryl), 5.88 (s, 1H, OH), 11.2 (s, 1H, −CHO); ^{13}C NMR (75.45 MHz; $CDCl_3$; Me_4Si at 25°C, ppm) $\delta = 105.3$ (−C1), 132.1 (−C2), 103.9 (−C3), 164.6 (−C4), 188.8 (−C10). IR (ν_{max}, cm^{-1}, KBr): 3425 (νOH), 2915 ($\nu as_{(C-H)}$, CH_2), 2865 ($\nu s_{(C-H)}$, CH_2), 1620 ($\nu_{CH=0}$), 1275 (ν_{C-O}).

2.3.7. Synthesis of N-(4-*n*-hexyloxysalicylidene)-4′-*n*-propylaniline, 4-6-3. An ethanolic solution of 2-hydroxy-(4-hexyloxy)-salicylaldehyde (0.22 g, 1 mmol) was added to an ethanolic solution of 4-*n*-propylaniline (0.13 g, 1 mmol). The solution mixture was refluxed with a few drops of acetic acid as catalyst for 3 h to yield the yellow Schiff base N-(4-*n*-hexyloxysalicylidene))-4′-*n*-propylaniline. The precipitate was collected by filtration and recrystallized several times from absolute ethanol to give a pure compound.

Yield: 0.26 g, 78%. Anal. Calcd for $C_{22}H_{29}NO_2$: FAB mass (*m*/*e*, fragment): *m*/*z*: calcd 339.2; found: 340 [M + H$^+$]; ^{1}H NMR (400 MHz, $CDCl_3$): δ 0.88 (t, $J = 6.8$ Hz, 6H, CH_3), 0.93–1.8 (m, 8H, $(-CH_2)_4$), 2.6 (t, $J = 7.4$ Hz, 2H, Ph–CH_2), 3.95 (t, $J = 6.7$ Hz, 2H, $-OCH_2$), 7.1–7.2 (m, 7-ArH), 8.21 (s, 1H, CH = N), 13.7 (s, 1H, OH). ^{13}C NMR (75.45 MHz; $CDCl_3$; Me_4Si at 25°C, ppm) $\delta = 161.3$ (−C1), 107.1 (−C2), 102.9 (−C3), 162.6 (−C4), 110.8 (−C5), 121.7 (−C6), 128.9 (−C7), 122.5 (−C8), 129.7 (−C9). IR (ν_{max}, cm^{-1}, KBr): 3435 (ν_{OH}), 2920 ($\nu_{as(C-H)}CH_2$), 2855 ($\nu_{s(C-H)}CH_2$), 1625 ($\nu_{C=N}$), 1285 (ν_{C-O}).

2.3.8. N-(4-*n*-decyloxysalicylidene)-4′-*n*-propylaniline, 4-10-3. Yield: 0.36 g, 78%. Anal. Calcd for $C_{26}H_{37}NO_2$: FAB mass (*m*/*e*, fragment): *m*/*z*: calcd 395.1; found: 396 [M + H$^+$]; ^{1}H NMR (400 MHz, $CDCl_3$): δ 0.88 (t, $J = 6.8$ Hz, 6H, CH_3), 0.93–1.8 (m, 16H, $(CH_2)_8$), 2.6 (t, $J = 7.6$ Hz, Ph–CH_2, 2H), 3.97 (t, $J = 6.8$ Hz, 2H, $-OCH_2$), 7.2–7.4 (m, 7-ArH), 8.5 (s, 1H, CH = N), 13.9 (s, 1H, OH). IR (ν_{max}, cm^{-1}, KBr): 3435 (ν_{OH}), 2920 ($\nu_{as(C-H)}CH_2$), 2850 ($\nu_{s(C-H)}CH_2$), 1625 ($\nu_{C=N}$), 1285 (ν_{C-O}).

2.3.9. N-(4-*n*-tetradecyloxysalicylidene)-4′-*n*-propylaniline, 4-14-3. Yield: 0.35 g, 78%. Anal. Calcd for $C_{30}H_{45}NO_2$: FAB mass (*m*/*e*, fragment): *m*/*z*: calcd 451.3; found: 452 [M + H$^+$]; ^{1}H NMR (400 MHz, $CDCl_3$): δ 0.89 (t, $J = 6.8$ Hz, 6H, CH_3), 0.94–1.8 (m, 22H, $(CH_2)_{11}$), 2.7 (t, $J = 7.4$ Hz, Ph–CH_2, 2H), 3.97 (t, $J = 6.7$ Hz, 2H, $-OCH_2$), 7.1–7.2 (m, 7-ArH), 8.4 (s, 1H, CH = N), 13.8 (s, 1H, OH). IR (ν_{max}, cm^{-1}, KBr): 3430 (ν_{OH}), 2925 ($\nu_{as(C-H)}CH_2$), 2850 ($\nu_{s(C-H)}CH_2$), 1625 ($\nu_{C=N}$), 1285 (ν_{C-O}).

2.3.10. N-(4-*n*-hexadecyloxysalicylidene)-4′-*n*-propylaniline, 4-16-3. Yield: 0.42 g, 80%. Anal. Calcd for $C_{32}H_{49}NO_2$: FAB mass (*m*/*e*, fragment): *m*/*z*: calcd 479.3; found: 480 [M + H$^+$]; ^{1}H NMR (400 MHz, $CDCl_3$): δ 0.91 (t, $J = 6.7$ Hz, 6H, CH_3), 0.94–1.8 (m, 28H, $(CH_2)_{14}$), 2.5 (t, $J = 7.4$ Hz, Ph–CH_2, 2H), 3.98 (t, $J = 6.7$ Hz, 2H, $-OCH_2$), 7.1–7.2 (m, 7-ArH), 8.5 (s, 1H, CH = N), 13.2 (s, 1H, OH). IR (ν_{max}, cm^{-1}, KBr): 3435 (ν_{OH}), 2920 ($\nu_{as(C-H)}CH_3$), 2855 ($\nu_{s(C-H)}CH_3$), 1625 ($\nu_{C=N}$), 1285 (ν_{C-O}).

2.3.11. N-(4-*n*-octaadecyloxysalicylidene)-4′-*n*-propylaniline, 4-18-3. Yield: 0.42 g, 80%. Anal. Calcd for $C_{34}H_{53}NO_2$: C, 80.4; H, 10.5; N, 2.7. FAB mass (*m*/*e*, fragment):

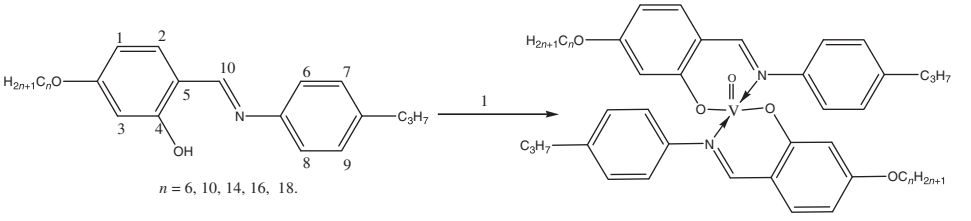

Scheme 2. 1: $VOSO_4 \cdot 5H_2O$, MeOH, TEA, Δ, 1 h.

m/z: calcd 507.4; found: 508 $[M + H^+]$; ^1H NMR (400 MHz, $CDCl_3$): δ 0.92 (t, $J = 6.7$ Hz, 6H, CH_3), 0.93–1.81 (m, 32H, $(CH_2)_{16}$), 2.54 (t, $J = 7.4$ Hz, Ph–CH_2, 2H), 3.99 (t, $J = 6.7$ Hz, 2H, $-OCH_2$), 7.1–7.2 (m, 7-ArH), 8.51 (s, 1H, CH = N), 13.22 (s, 1H, OH). IR (ν_{max}, cm^{-1}, KBr): 3435 (ν_{OH}), 2925 ($\nu_{as(C-H)}CH_3$), 2855 ($\nu_{s(C-H)}CH_3$), 1625 ($\nu_{C=N}$), 1285 (ν_{C-O}).

2.4. *Synthesis of oxovanadium(IV) complexes*

To the ligand 4-6-3 (0.33 g, 1 mmol) or 4-10-3 (0.39 g, 1 mmol) or 4-14-3 (0.45 g, 1 mmol) or 4-16-3 (0.47 g, 1 mmol) or 4-18-3 (0.50 g, 1 mmol) dissolved in minimum volume of absolute ethanol vanadyl sulfate $VOSO_4 \cdot 5H_2O$ (0.11 g, 0.5 mmol) in methanol was added followed by the addition of triethylamine and refluxed for 2 h, scheme 2. A greenish solid formed immediately, was filtered, washed with diethyl ether, and recrystallized from chloroform–ethanol.

2.4.1. Oxovanadium(IV) complex, (VO-6-3). Yield: 0.35 g (75%) Anal. Calcd for $C_{44}H_{56}N_2O_5V$: FAB mass (*m/e*, fragment): *m/z*: calcd 743.3; found: 744 $[M + H^+]$; IR (KBr, cm^{-1}): 1610 (νC = N), 1135 (νC–O, phenolic), 975 (νV=O).

2.4.2. Oxovanadium(IV) complex, (VO-10-3). Yield: 0.35 g (70%) Anal. Calcd for $C_{52}H_{72}N_2O_5V$: FAB mass (*m/e*, fragment): *m/z*: calcd 855.4; found: 856 $[M + H^+]$; IR (KBr, cm^{-1}): 1610 (νC=N), 1135 (νC–O, phenolic), 970 (νV=O).

2.4.3. Oxovanadium(IV) complex, (VO-14-3). Yield: 0.37 g (75%) Anal. Calcd for $C_{60}H_{88}N_2O_5V$: FAB mass (*m/e*, fragment): *m/z*: calcd 967.6; found: 968 $[M + H^+]$; IR (KBr, cm^{-1}): 1610 (νC=N), 1135 (νC–O, phenolic), 965 (νV=O).

2.4.4. Oxovanadium(IV) complex, (VO-16-3). Yield: 0.39 g (78%) Anal. Calcd for $C_{64}H_{96}N_2O_5V$: FAB mass (*m/e*, fragment): *m/z*: calcd 1023.6; found: 1024 $[M + H^+]$; IR (KBr, cm^{-1}): 1615 (νC=N), 1135 (νC–O, phenolic), 975 (νV=O).

2.4.5. Oxovanadium(IV) complex, (VO-18-3). Yield: 0.39 g (78%) Anal. Calcd for $C_{68}H_{104}N_2O_5V$: FAB mass (*m/e*, fragment): *m/z*: calcd 1079.7; found: 1080 $[M + H^+]$; IR (KBr, cm^{-1}): 1614 (νC=N), 1130 (νC–O, phenolic), 968 (νV=O).

Table 1. Analytical data of the compounds.

Compounds	C (%)	H (%)	N (%)	UV-Vis λ_{max} (nm) (ε, mol l^{-1} cm^{-1}) (Transition)	IR (cm^{-1})	FAB mass
$C_{22}H_{29}NO_2$ (4-6-3)	78.8 (78.7)	8.4 (8.6)	4.2 (4.1)	245 (3500) ($\pi \rightarrow \pi^*$) 294 (2900) ($\pi \rightarrow \pi^*$) 338 (2400) ($\pi \rightarrow \pi^*$)	1627 ($\nu_{C=N}$) 3431 (ν_{OH})	340
$C_{44}H_{56}N_2O_5V$ (VO-6-3)	71.1 (71.0)	7.4 (7.5)	3.6 (3.5)	244 (5400) ($\pi \rightarrow \pi^*$) 325 (2200) ($\pi \rightarrow \pi^*$) 398 (2500) (MLCT) 457 (700) (d–d)	1612 ($\nu_{C=N}$) 970 ($\nu_{V=O}$) 532 (ν_{M-N}) 461 (ν_{M-O})	744
$C_{26}H_{37}NO_2$ (4-10-3)	79.1 (78.9)	9.3 (9.4)	3.6 (3.5)	245 (3500) ($\pi \rightarrow \pi^*$) 294 (2900) ($\pi \rightarrow \pi^*$) 338 (2400) ($\pi \rightarrow \pi^*$)	1629 ($\nu_{C=N}$) 3433 (ν_{OH})	396
$C_{52}H_{72}N_2O_5V$ (VO-10-3)	72.8 (72.9)	8.5 (8.4)	3.1 (3.2)	243 (5400) ($\pi \rightarrow \pi^*$) 324 (2200) ($\pi \rightarrow \pi^*$) 399 (2500) (MLCT) 456 (697) (d–d)	1610 ($\nu_{C=N}$) 970 ($\nu_{V=O}$) 531 (ν_{M-N}) 457 (ν_{M-O})	856
$C_{30}H_{45}NO_2$ (4-14-3)	79.8 (79.7)	10.1 (10.0)	3.2 (3.1)	245 (3500) ($\pi \rightarrow \pi^*$) 294 (2900) ($\pi \rightarrow \pi^*$) 337 (2400) ($\pi \rightarrow \pi^*$)	1628 ($\nu_{C=N}$) 3432 (ν_{OH})	452
$C_{60}H_{88}N_2O_5V$ (VO-14-3)	74.3 (74.4)	9.2 (9.1)	2.7 (2.8)	242 (5400) ($\pi \rightarrow \pi^*$) 322 (2200) ($\pi \rightarrow \pi^*$) 397 (2500) (MLCT) 455 (697) (d–d)	1606 ($\nu_{C=N}$) 969 ($\nu_{V=O}$) 532 (ν_{M-N}) 458 (ν_{M-O})	968
$C_{32}H_{49}NO_2$ (4-16-3)	80.2 (80.1)	10.4 (10.3)	2.8 (2.9)	245 (3500) ($\pi \rightarrow \pi^*$) 294 (2900) ($\pi \rightarrow \pi^*$) 337 (2400) ($\pi \rightarrow \pi^*$)	1627 ($\nu_{C=N}$) 3431 (ν_{OH})	480
$C_{64}H_{96}N_2O_5V$ (VO-16-3)	75.1 (75.0)	9.3 (9.4)	2.8 (2.7)	242 (5400) ($\pi \rightarrow \pi^*$) 322 (2200) ($\pi \rightarrow \pi^*$) 397 (2500) (MLCT) 455 (697) (d–d)	1616 ($\nu_{C=N}$) 971 ($\nu_{V=O}$) 531 (ν_{M-N}) 453 (ν_{M-O})	1024
$C_{34}H_{52}NO_2$ (4-18-3)	80.4 (80.2)	10.5 (10.4)	2.7 (2.8)	245 (3500) ($\pi \rightarrow \pi^*$) 294 (2900) ($\pi \rightarrow \pi^*$) 337 (2400) ($\pi \rightarrow \pi^*$)	1626 ($\nu_{C=N}$) 3432 (ν_{OH})	508
$C_{68}H_{104}N_2O_5V$ (VO-18-3)	75.4 (75.5)	9.6 (9.7)	2.6 (2.5)	247 (5400) ($\pi \rightarrow \pi^*$) 321 (2200) ($\pi \rightarrow \pi^*$) 395 (2500) (MLCT) 453 (697) (d–d)	1614 ($\nu_{C=N}$) 968 ($\nu_{V=O}$) 531 (ν_{M-N}) 453 (ν_{M-O})	1080

3. Results and discussion

3.1. *Spectral investigation*

Characterization of the compounds was done by elemental analyses, FT-IR, UV-Vis, ^{1}H-NMR, and mass spectrometries (table 1). The analytical data are in good agreement with the proposed formulae. The Schiff bases exhibited ν_{CN} at 1635–1625 cm^{-1}; this band shifts to a lower wavenumber (1610–1620 cm^{-1}) upon chelation, reflecting coordination of azomethine. Occurrence of vanadyl (V=O) stretching mode at 975 cm^{-1} indicates the absence of intermolecular ($\cdots$V=O$\cdots$V=O$\cdots$) interaction confirming monomeric complexes [48–50]. The appearance of additional bands at 465–480 and 525–545 cm^{-1} (table 1) in spectra of the complexes assigned to V−O and V–N stretches that are not observed in spectra of the ligands furnished evidence for [N, O] binding of the ligand. The ^{1}H NMR spectra of ligands show signal at 13.4–13.8 ppm, corresponding to the proton of OH. The imine group is at 8.5 ppm. FAB-mass spectra

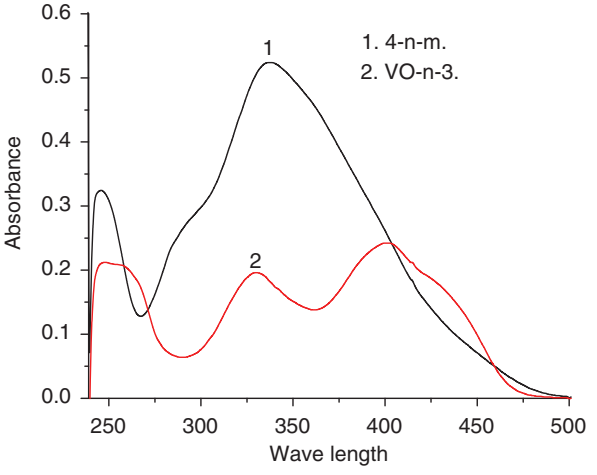

Figure 2. UV-Vis spectra of 4-n-m and VO-n-3.

Table 2. Phase transition temperatures (T, °C), associated enthalpies (ΔH, kJ mol^{-1}) of 4-n-3 and their complexes.

Compounds	Heating	Cooling
4-6-10	Cr 42.3 (0.7)N92.6 (0.7)I	I 91.5 (0.8)N41.7 (0.5)Cr
4-10-3	Cr 43.5 (28.9)SmC68.4 (0.2)N91.7 (1.0)I	I 90.8 (1.1)N67.6 (0.2)SmC
4-14-3	Cr 59.5 (45.1)SmC83.6 (0.3)N88.1 (1.8)I	I 87.1 (1.8)N82.8 (0.2)SmC
4-16-3	Cr 66.1 (51.2)SmC84.2 (0.7)N85.8 (1.9)I	I 85.3 (2.1)N83.9 (0.5) SmC (49.1) Cr
4-18-3	Cr 72.6 (55.4)SmA84.9 (4.7)I	I 83.8 (4.8)SmA59.2 (45.2)Cr
VO-6-3	Cr 191.5 (10.6)I	I 161.5 (1.7)N 153.9 (0.9)Cr
VO-10-3	Cr 83.6 (39.5)SmA97.6 (34.8) SmE171.3 (126.2)I	I 167.6 (37.5)SmA128.8 (40.7)SmE
VO-14-3	Cr 97.7 (26.4)SmA150.0 (4.8)I	I 150.0 (3.7)SmA76.6 (8.9)Cr
VO-16-3	Cr 101.8 (78.9)SmA145.4 (7.1) SmE155.9 (8.4)I	I 154.3 (7.7)SmA116.1 (8.1) SmE87.8 (16.1)Cr
VO-18-3	Cr 88.6 (44.9) SmA98.2 (5.1)	–

of the vanadyl(IV) complexes are in agreement with their formula weights (table 1). Electronic absorption spectra (figure 2) of the ligand (4-18-3) exhibited bands at ~246 nm ($\varepsilon = 3400$ L mol^{-1} cm^{-1}) and ~295 nm ($\varepsilon = 2900$ L mol^{-1} cm^{-1}) due to $\pi - \pi^*$ intra-ligand transitions of the aromatic rings and at ~337 nm ($\varepsilon = 5400$ L mol^{-1} cm^{-1}) for $\pi - \pi^*$ transition of imine (−C=N) chromophores. The latter band is blue shifted to ~328 nm on complexation (figure 2). In addition, low intensity bands at ~400 nm ($\varepsilon = 2400$ L mol^{-1} cm^{-1}) for vanadyl(IV) complex (5-18-3) are assigned to LMCT transition. A weak shoulder appeared at 455 nm in VO-18-3 ($\varepsilon = 700$ L mol^{-1} cm^{-1}), attributed to d–d transition. A rather similar observation (table 1) was also noted for other compounds.

3.2. *Electrochemical behavior*

The electrochemical behavior of a representative complex (VO-18-3) was probed by cyclic voltammetry in acetonitrile solution from −1.2 to 1.2 V *versus* SCE electrode. The

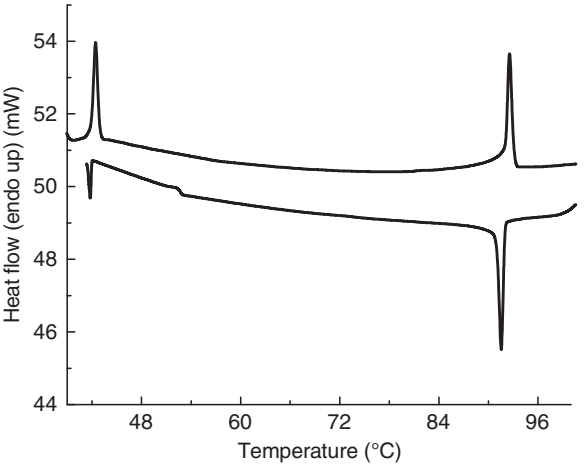

Figure 3. DSC thermogram of 4-6-3.

voltammogram (Supplementary material) displayed a quasireversible (peak-to-peak separation >100 mV) cyclic voltammetric response due to VO^{3+}/VO^{2+} couple at ($E_{1/2} = +0.60$ V, $E_p^c = 0.39$ V, $E_p^a = 0.82$ V, $\Delta E_p = 0.42$ V).

3.3. *Variable temperature magnetic susceptibility*

The variable temperature magnetic susceptibility measurements were carried out for a representative complex, VO-18-3. The effective magnetic moment is 1.73 B.M. corresponding to the d^1 configuration showing negligible electron exchange interactions. The effective magnetic moment of this complex did not vary appreciably in the range of experimental temperature and the complexes studied in this work exhibited a straight line when the inverse of the susceptibility is plotted against temperature (Supplementary material), satisfying Curie–Weiss equation.

3.4. *Mesomorphic behavior: polarizing optical microscopy and DSC studies*

The phase transitions of the compounds were monitored using DSC and polarizing optical microscopy (POM). Both the ligands and their complexes exhibit liquid-crystalline behavior. The thermal behavior of the ligands and complexes are given in table 2. Thermodynamic phase transitions and types of mesophases were identified by characteristic optical textures observed in a thermal polarizing microscope and enthalpy values in DSC thermograms. The DSC traces (figure 3) of compound 4-6-3 (scheme 1) exhibited a highly thermally stable transition with a very low enthalpy value ($\Delta H = 0.81$ kJ mol^{-1}) owing to the I-N mesophase transition. The POM study revealed a schlieren texture of the N phase (figure 4). The DSC study for compound 4-10-3 showed three transitions on heating cycle and two transitions on cooling cycle. The transition at 90.8°C ($\Delta H = 1.1$ kJ mol^{-1}) is due to the isotropic-nematic phase, and that at 67.6°C ($\Delta H = 1.1$ kJ mol^{-1}) is due to the nematic-smectic C phase. No transition from mesophase to crystalline phase was observed in the DSC during cooling,

presumably due to slower transition to the more organized phases, and partial or complete vitrification of compounds upon cooling [49]. On slow cooling, schlieren texture of the N phase was observed at 90°C, which on further cooling produced a schlieren texture of the SmC phase with four brush defects (figure 5) at 67°C. The compound solidified at 37°C. A similar observation was noted for compound 4-14-3. Compound 4-16-3 displayed three transitions on heating as well as in cooling cycles (figure 6). The transition at 85.3°C ($\Delta H = 2.1\,\mathrm{kJ\,mol^{-1}}$) is due to the isotropic to the N phase and at 83.9°C ($\Delta H = 1.4\,\mathrm{kJ\,mol^{-1}}$) is from the N to the SmC phase. The POM observation is quite similar to 4-10-3. Quite surprisingly, compound 4-18-3 showed the SmA mesophase at ~84°C. The DSC study also exhibited two transition in heating and two in cooling cycle. The higher enthalpies for the SmA mesophase are consistent with other reported systems [47, 48]. On the whole mesophase to isotropic transition temperature decreases with increase in carbon chain length (figure 7). The complexes (VO-n-3) with higher alkoxy carbon chain length ($n = 10, 14, 16$, and 18) showed the SmA and/or the smectic E phase. On slow cooling the sample showed a high

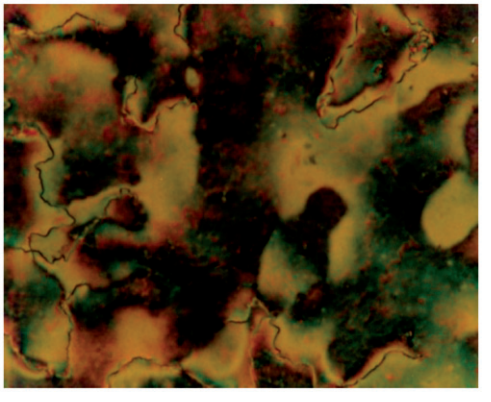

Figure 4. Schlieren texture of the N phase.

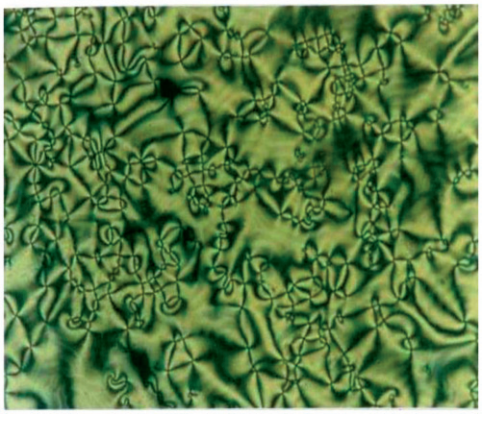

Figure 5. Schlieren texture of the SmC phase.

birefringent fan-like texture of the SmA phase at ~167–96°C (figure 8), which on further cooling showed arced fan-like textures of the smectic E phase at 116–128°C (figure 9). The smectic A–smectic E phase transitions cannot be detected for VO-14-3 and VO-18-3 in DSC. VO-18-3 showed monotropic transition in DSC. Among the compounds VO-6-3 was exceptional in showing the N phase (figure 10). This is not quite ubiquitous for related systems. The mesophase stability, however, is very low and quickly transcend to solid state. The DSC study is also concordant with this observation. DSC thermograms for VO-16-3 and VO-6-3 are shown in figures 11 and 12, respectively. Pertinent here is to mention that all previously reported analogous metallomesogens showed smectic mesomorphism [46–48]. A plot of transition temperature *versus* the number of carbons in the alkoxy chain (figure 13) shows that the mesophase to isotropic transition temperature and vice versa for the complexes did not show any definite trend.

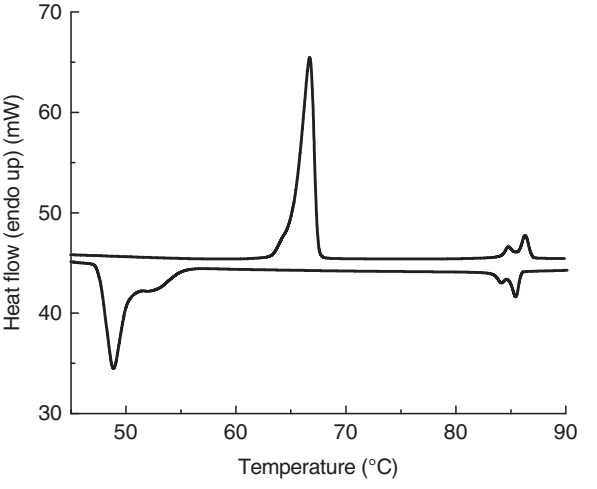

Figure 6. DSC thermogram of 4-16-3.

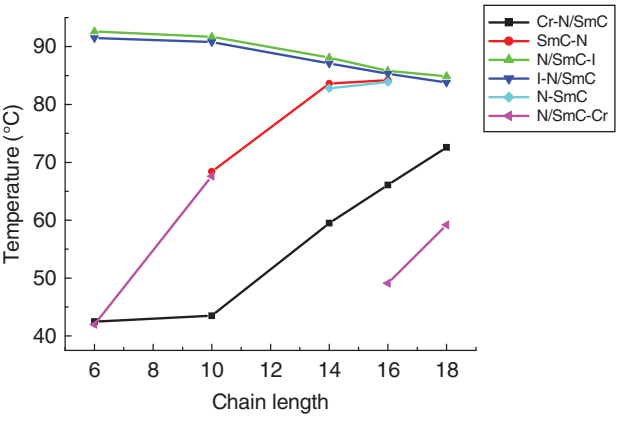

Figure 7. Variation of carbon chain length with transition temperature in 4-n-m.

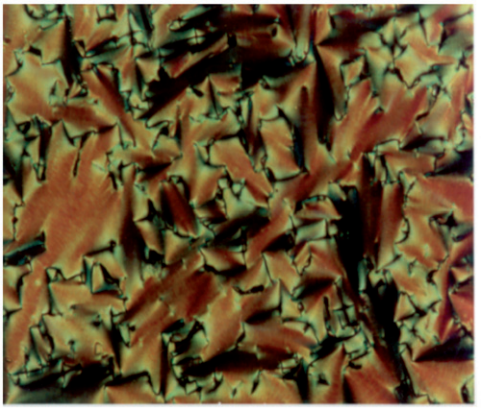

Figure 8. Fan-like texture of the SmA phase.

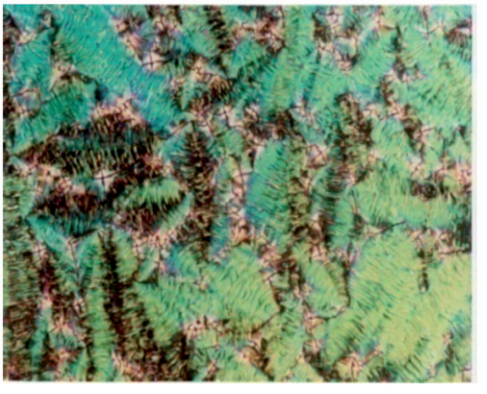

Figure 9. Texture of the SmE phase.

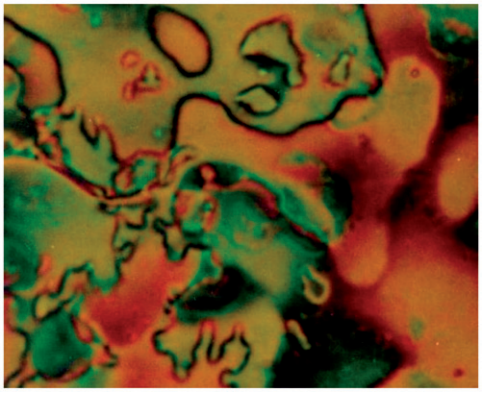

Figure 10. Schlieren texture of the N phase.

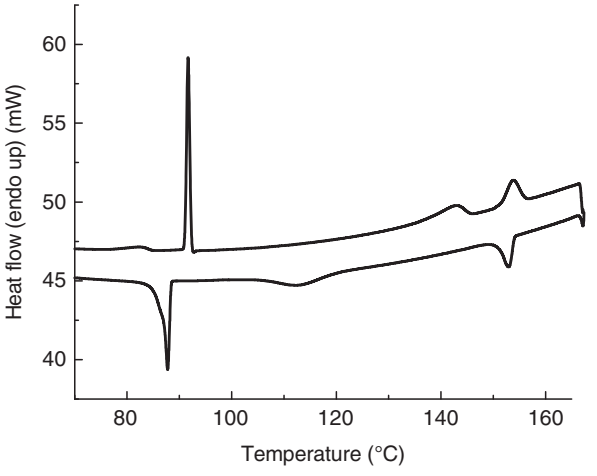

Figure 11. DSC thermogram of VO-16-3.

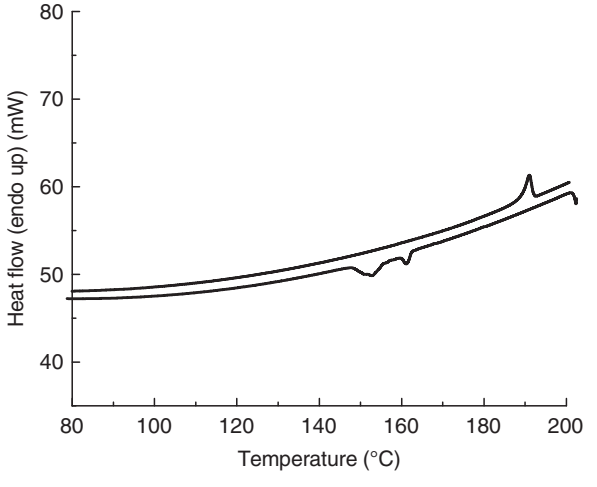

Figure 12. DSC thermogram of VO-6-3.

3.5. *Density functional theory study*

As suitable X-ray quality crystal could not be grown, density functional theory (DFT) calculation has been performed to investigate the electronic structure of the V(IV) complexes (figure 14). Full geometry optimization has been carried out without imposing any constrain with the DMol3 program package [51]. Spin-unrestricted DFT calculation has been carried out in the framework of the generalized gradient approximation (GGA). At the GGA level, we have chosen the BLYP functional [52–56] which incorporates Becke's exchange crystal functions as the double-numerical

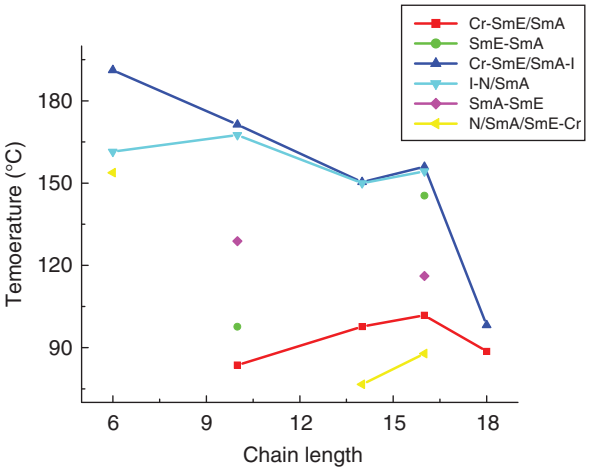

Figure 13. Variation of carbon chain length with transition temperature in VO-n-m.

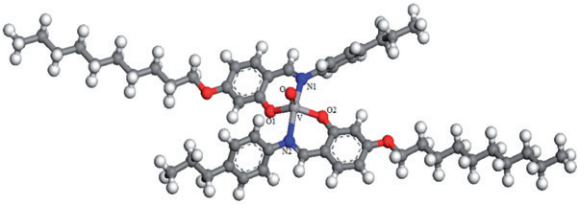

Figure 14. Optimized structure of VO-10-3.

atomic orbitals augmented by polarization functions, i.e., functions with angular momentum one higher than that of the highest occupied orbital in the free atom. The size is comparable with the Gaussian 6-31 G** basis set, but the DNP basis set is supposed to be more accurate than a Gaussian basis set of similar size. In our calculations, self-consistent field procedures are performed with a convergence criterion of 2×10^{-5} a.u. on the total energy and 10^{-6} a.u. on electron density.

The 3-D iso-surface plots of the highest occupied molecular orbital (HOMO) and lowest unoccupied molecular orbital (LUMO) of the complex are shown (figures 15 and 16). The HOMO and LUMO energies are calculated to be −3.925 eV and −2.350 eV, respectively, $\Delta E = 1.575$ eV. The HOMO–LUMO energy separation can be used as a measure of kinetic stability of the molecule and could indicate the reactivity pattern [57, 58]. A large HOMO–LUMO gap implies a high-kinetic stability and low-chemical reactivity, because it is energetically unfavorable to add electrons to a high-lying LUMO or to extract electrons from a low-lying HOMO [58]. The HOMO–LUMO energy gap of 1.575 eV suggests that the complex is fairly stable. Some of the selective geometric parameters of optimized vanadyl complex evaluated by the DFT calculation at the BLYP/DNP level are shown in table 3. The calculated average V–O and V–N bond lengths of VO-10-3 are 1.954 and 2.18 Å, respectively, and V=O bond length

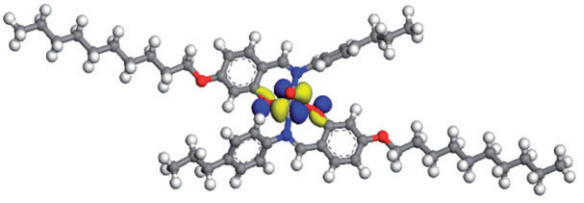

Figure 15. HOMO energy diagram of VO-10-3.

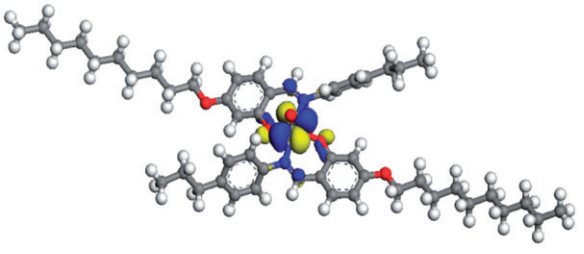

Figure 16. LUMO energy diagram of VO-10-3.

Table 3. Selected bond lengths (Å) and bond angles (°) of VO-10-3 optimized at the BLYP/DNP level of theory.

Structural parameters	VO-10-3
V–O(1)	1.953
V–O(2)	1.956
V–O	1.621
V–N(1)	2.178
V–N(2)	2.179
O(1)–V–O(2)	130.5
N(1)–V–N(2)	161.0
N(1)–V–O(2)	85.7
O(1)–V–N(1)	86.3
O(1)–V–N(2)	86.0
N(2)–V–O(2)	86.3

1.621 Å. The bond angles 130.5° and 161.0° for O1–VO–O2 and N1–VO–N2, respectively, around the vanadium atom indicate a square-pyramidal geometry.

4. Conclusion

A systematic investigation on a series of oxovanadium(IV) complexes of bidentate [N, O] donor Schiff base have been carried out. All the compounds are mesogenic. The complexes with higher carbon chain length exhibit smectic mesomorphism whereas shorter carbon chain length ($n = 6$) showed nematic mesophase. Mesophase to isotropic

transition temperature decreases with increase in chain length. Cyclic voltammetry reveals a quasireversible one-electron response for the VO(V)/VO(IV) redox couple. Based on the spectral results and DFT study a five-coordinate, square-pyramidal structure has been suggested.

Acknowledgments

The authors thank SAIF, NEHU, and CDRI, Lucknow for analytical and spectral data. GD acknowledges the financial support from DST and UGC, Government of India. Dr R.C. Deka, Tezpur University, India, is acknowledged for computational facility.

References

[1] N. Hoshino. *Coord. Chem. Rev.*, **174**, 77 (1998).
[2] J.L. Serrano. *Metallomesogens*, Wiley-VCH, Weinheim (1996).
[3] B. Donnio, D. Guillon, R. Deschenaux, D.W. Bruce. In *Comprehensive Coordination Chemistry II*, J.A. McCleverty, T.J. Meyer (Eds), pp. 357–627, Elsevier, Oxford (2003).
[4] A.M. Giroud-Godquin, P.M. Maitlis. *Angew. Chem., Int. Ed. Engl.*, **30**, 375 (1991).
[5] P. Espinet, M.A. Esteruelas, L.A. Oro, J.L. Serrano, E. Sola. *Coord. Chem. Rev.*, **117**, 215 (1992).
[6] S.A. Hudson, P.M. Maitlis. *Chem. Rev.*, **93**, 861 (1993).
[7] A. Polishchuk, T.V. Timofeeva. *Russ. Chem. Rev.*, **62**, 291 (1993).
[8] D.W. Bruce. In *Inorganic Materials*, D.W. Bruce, D. O'Hare (Eds), p. 429, Wiley, Chichester (1996).
[9] F. Neve. *Adv. Mater.*, **8**, 277 (1996).
[10] S.R. Collinson, D.W. Bruce. In *Transition Metals in Supramolecular Chemistry*, J.P. Sauvage (Ed.), p. 285, Wiley, New York (1999).
[11] V.A. Molochko, N.S. Rukk. *Russ. J. Coord. Chem.*, **26**, 829 (2000).
[12] K. Binnemans, C. Gorller-Walrand. *Chem. Rev.*, **102**, 2303 (2002).
[13] B. Donnio, D. Guillon, D.W. Bruce, R. Deschenaux. In *Comprehensive Coordination Chemistry II: From Biology to Nanotechnology*, J.A. McCleverty, T.J. Meyer, M. Fujita, A. Powell (Eds), Vol. 7, pp. 357–627, Elsevier, Oxford, UK (2003).
[14] R.W. Date, E.F. Iglesias, K.E. Rowe, J.M. Elliott, D.W. Bruce. *Dalton Trans.*, 1914 (2003).
[15] K. Nejati, Z. Rezvani, E. Alizadeh, R. Sammimi. *J. Coord. Chem.*, **64**, 1859 (2011).
[16] C.K. Lai, C.-H. Chang, C.-H. Tsai. *J. Mater. Chem.*, **17**, 2319 (2007).
[17] J. Barbera, A.M. Levelut, M. Marcos, P. Romero, J.L. Serrano. *Liq. Cryst.*, **10**, 119 (1991).
[18] J. Barbera, R. Gimenez, N. Gimeno, M. Marcos, M.D.C. Pina, J.L. Serrano. *Liq. Cryst.*, **30**, 651 (2003).
[19] A. Butler, J.V. Walker. *Chem. Rev.*, **93**, 1937 (1993).
[20] N. Muhammad, S. Ali, S. Shahzadi, A.N. Khan. *Russ. J. Coord. Chem.*, **34**, 448 (2008).
[21] Z.H. Chohan, S.H. Sumrra, M.H. Youssoufi, T.B. Hadda. *J. Coord. Chem.*, **63**, 3981 (2010).
[22] P. Noblia, M. Vieites, B.S. Parajon-Costa, E.J. Baran, H. Cerecetto, P. Draper, M. Gonzalez, O.E. Piro, E.E. Castellano, A. Azqueta, A. Lopez de Cerain, A. Monge-Vega, D. Gambino. *J. Inorg. Biochem.*, **99**, 443 (2005).
[23] Y. Dong, R.K. Narla, E. Sudbeck, F.M. Uckun. *J. Inorg. Biochem.*, **78**, 321 (2000).
[24] O.J.D. Cruz, Y. Dong, F.M. Uckun. *Bio. Reprod.*, **60**, 435 (1999).
[25] H. Sakurai, Y. Kojitane, Y. Yoshikawa, K. Kawabe, H. Yasui. *Coord. Chem. Rev.*, **226**, 187 (2002).
[26] Yu.G. Galyametdinov, I.G. Bikchantaev, I.V. Ovchinnikov. *Zh. Obshch. Khim.*, **58**, 1326 (1988).
[27] J. Mohebbi, S. Nikpour, S. Rayati. *J. Mol. Catal. A*, **256**, 265 (2006).
[28] A. Butler, C.J. Carrano. *Coord. Chem. Rev.*, **109**, 152 (1991).
[29] Y. Masuda. *Thermochim. Acta*, **60**, 203 (1983).
[30] G.L. Jeyaraj, J.E. House Jr. *Thermochim. Acta*, **66**, 289 (1983).
[31] I. Teucher, C.M. Paleos, M.M. Labes. *Mol. Cryst. Liq. Cryst.*, **11**, 187 (1970).
[32] A.K. Prajapati, N. Bonde. *Liq. Cryst.*, **33**, 1189 (2006).
[33] Z. Rezvani, K. Nejati, M. Seyedahmadian, B. Divband. *Mol. Cryst. Liq. Cryst.*, **493**, 71 (2008).
[34] A.S. Mocanu, M. Ilis, F. Dumitrascu, M. Ilie, V. Circu. *Inorg. Chim. Acta*, **363**, 729 (2010).

[35] U. Caruso, R. Diana, B. Panunzi, A. Roviello, M. Tingoli, A. Tuzi. *Inorg. Chem. Commun.*, **12**, 1135 (2009).
[36] S. Hayami, K. Danjobara, S. Miyazaki, K. Inoue, Y. Ogawa, Y. Maeda. *Polyhedron*, **24**, 2821 (2005).
[37] O.N. Kadkin, E.H. Kim, Y.J. Rha, S.Y. Kim, J. Tae, M.-G. Choi. *Chem. Eur. J.*, **15**, 10343 (2009).
[38] S. Hayami, N. Motokawa, A. Shuto, N. Masuhara, T. Someya, Y. Ogawa, K. Inoue, Y. Maeda. *Inorg. Chem.*, **46**, 1789 (2007).
[39] F. Morale, R.L. Finn, S.R. Collinson, A.J. Blake, C. Wilson, D.W. Bruce, D. Guillon, B. Donnio, M. Schroder. *New J. Chem.*, **32**, 297 (2008).
[40] C.R. Bhattacharjee, G. Das, P. Mondal, S.K. Prasad, D.S.S. Rao. *Inorg. Chem. Commun.*, **14**, 606 (2011).
[41] C.R. Bhattacharjee, G. Das, P. Mondal, S.K. Prasad, D.S.S. Rao. *Liq. Cryst.*, **38**, 615 (2011).
[42] I.V. Ovchinnikov, Yu.G. Galyametdinov, G.I. Ivanova, L.M. Yagfarova. *Dokl. Akad. Nauk. SSSR*, **276**, 126 (1984).
[43] M. Ghedini, S. Armentano, R. Bartolino, N. Kirov, M. Petrov, S. Nenova. *J. Mol. Liq.*, **38**, 207 (1988).
[44] G. Torquati, O. Francescangeli, M. Ghedini, S. Armentano, F.P. Nicoletta, R. Bartolino. *Il Nuovo Cim.*, **12**, 1363 (1990).
[45] R. Bartolino, F. Rustichelli, N. Scaramuzza, C.C. Versace, M. Ghedini, M.C. Pagnotta, S. Armentano, M.A. Ricci, P. Benassi. *Solid State Commun.*, **80**, 587 (1991).
[46] M. Ghedini, S. Morrone, D. Gatteschi, C. Znachini. *Chem. Mater.*, **3**, 752 (1991).
[47] M. Ghedini, S. Morrone, R. Bartolino, V. Formoso, O. Francescangeli, B. Yang, D. Gatteschi, C. Znachini. *Chem. Mater.*, **5**, 876 (1993).
[48] C.R. Bhattacharjee, G. Das, D.D. Purkayastha, P. Mondal. *Liq. Cryst.*, **38**, 717 (2011).
[49] C.R. Bhattacharjee, G. Das, D.D. Purkayastha, P. Mondal, P. Kanoo. *J. Coord. Chem.*, **64**, 2746 (2011).
[50] M.R. Maurya. *Coord. Chem. Rev.*, **237**, 163 (2003).
[51] B. Delley. *J. Chem. Phys.*, **92**, 508 (1990).
[52] P. Hohenberg, W. Kohn. *Phys. Rev. B*, **136**, 864 (1964).
[53] W. Kohn, L. Sham. *Phys. Rev. A*, **140**, 1133 (1965).
[54] A.D. Becke. *Phys. Rev. A*, **38**, 3098 (1988).
[55] C. Lee, W. Yang, R.G. Parr. *Phys. Rev. B*, **37**, 785 (1988).
[56] B. Delly, D.E. Ellis. *J. Chem. Phys.*, **76**, 1949 (1982).
[57] K.H. Kim, Y.K. Han, J. Jung. *Theor. Chem. Acc.*, **113**, 233 (2005).
[58] J. Aihara. *J. Phys. Chem. A*, **103**, 7487 (1999).